GEOPHYSICAL RESEARCH LETTERS, VOL. 29, NO. 10, PAGES **119**-1 – **119**-4 , 10.1029/2001GL013666, 2002

Propagation of auroral hiss at high altitudes

O. Santolík[1] and D. A. Gurnett

Department of Physics and Astronomy, University of Iowa, Iowa City.

Abstract. Using multicomponent wave measurements of the Polar spacecraft, we provide direct evidence of the propagation pattern of funnel-shaped auroral hiss at a radial distance of 5 Earth radii. The waves propagate upward and the Poynting flux is directed toward higher latitudes in the high-latitude part of the emission and to lower latitudes in the low-latitude part. The wave vectors are found to be close to the whistler mode resonance angle. Consistent with the theory, the latitudinal component of the wave vector is opposite compared to that of the Poynting flux in the low-latitude and high-latitude parts of the funnel-shaped emission. In the central part of the emission we observe a very broad distribution of the wave energy with respect to the azimuth angle. The waves thus simultaneously come from different directions with different wave vectors. This leads us to the conclusion that hiss is more likely generated in an extended sheet source rather than in a vertical line source or a point source. In this case the observed propagation pattern suggests that the sheet source is oriented roughly in the longitudinal direction, consistent with the region where we can expect presence of upgoing or counterstreaming electron beams.

1. Introduction

Auroral hiss is an intense plasma wave emission which frequently occurs in the high-latitude region of the Earth's magnetosphere [e.g., *Gurnett*, 1966; *Persoon et al.*, 1988; *Kasahara et al.*, 1995]. Observed by orbiting spacecraft it often appears with a characteristic funnel shaped envelope on time-frequency spectrograms (the lower-frequency cutoff first decreases and then increases). *Mosier and Gurnett* [1969] explained this envelope by a limitation of ray angles for whistler-mode waves propagating from a localized source. For a wave vector close to the resonance angle θ_R [*Stix*, 1992] the ray direction is perpendicular to the wave vector and the ray deviates from the static magnetic field ($\boldsymbol{B}_0$) by a complementary angle $\pi/2 - \theta_R$. Since the resonance cone closes with increasing frequency (θ_R decreases) the ray direction becomes more and more declined from $\boldsymbol{B}_0$. Waves at higher frequencies thus can propagate across the field lines to larger distances from the source than waves at lower frequencies, creating the observed funnel shaped envelope. *Gurnett and Frank* [1972] used this interpretation for downgoing auroral hiss observed at an altitude of 2500 km. Analysis of the envelope lead them to the conclusion that the waves come from a source in the auroral region at a radial distance of 1.8–2.6 Earth radii (R_E). They further associated the emission with downgoing low-energy electrons between 100 eV and several keV. At altitudes of 3000–6000 km *Kasahara et al.* [1995] reported downgoing hiss with wave vectors highly declined from $\boldsymbol{B}_0$. Their interpretation of the funnel shaped envelope assumed a line source extended up to radial distances of 2.9 R_E. *Gurnett et al.* [1983] measured electric field fluctuations at much higher altitudes corresponding to radial distances between 2.5 and 4 R_E. No direct measurement of Poynting flux was available but the observed upper cutoffs suggested that the waves were upgoing. Analysis of the envelope resulted in a radial distance of the source between 1.7 to 1.9 R_E.

The aim of this letter is to provide the first direct measurements of the wave normal and Poynting flux directions of funnel-shaped auroral hiss at high altitudes where we expect upgoing waves. We use measurements of the plasma wave instrument (PWI) onboard the Polar spacecraft [*Gurnett et al.*, 1995]. During the 1.5 year PWI operation period the satellite passed through the northern auroral region at a radial distance of 5 R_E, i.e., well above the expected source region of upgoing hiss. The case presented here was selected from 24 passes where PWI simultaneously measured vectors of magnetic and electric field fluctuations of auroral hiss in the high-rate telemetry mode, and where the magnetic component was sufficiently strong. We analyze simultaneous waveform measurements of electric and magnetic fields in the frequency range 230 Hz–20 kHz and we determine the Poynting flux and wave vector directions using both plane-wave methods and the wave distribution function (WDF) analysis [*Storey and Lefeuvre*, 1979].

2. Observations

Figure 1 shows results obtained from an analysis of data acquired on March 6, 1997 when the satellite moved on the night-side from the polar cap toward lower latitudes. The six-component waveforms were sampled at a rate of 71.4 samples per second and organized in snapshots of 0.445 s separated by gaps of 8.755 s. Figures 1a and 1b show spectrograms composed of sums of auto-power spectra of double-probe electric antennas and search-coil magnetic antennas, respectively. Data from each snapshot were processed separately and the data gaps were filled by the spectrum from the preceding snapshot. In the electric spectrogram (Figure 1a) we can easily find a funnel-shaped emission of auroral hiss centered around 0625 UT. On the high-latitude side the electric field spectra show a sharp high-frequency cutoff which can be identified with the local plasma frequency f_p [*Persoon et al.*, 1988]. The cutoff decreases by a factor of 3 in an auroral density cavity between 0620 and 0625 UT, and becomes diffuse and difficult to localise at lower latitudes after 0625 UT. The magnetic-field spectrogram in Figure 1b also displays parts of the funnel shape especially at lower latitudes. After 0645 UT a different type of emission is observed below $\sim$0.8 kHz. It is easily seen in the magnetic field data and possibly due to whistler-mode chorus. Similar spectra are simultaneously measured by the sweep frequency analyzer, using electric double-probe and magnetic loop antennas (not shown). This instrument also recorded a high-latitude extension of the funnel-shaped auroral hiss which was observed along the satellite orbit for about 2 hours before the interval shown in Figure 1. Emissions of auroral kilometric radiation were also simultaneously detected between 100 and 600 kHz.

[1]Now at Faculty of Mathematics and Physics, Charles University, Prague, and at Institute of Atmospheric Physics, Czech Academy of Sciences, Prague, Czech Republic.

Paper number 2001GL013666.
0094-8276/02/2001GL013666$5.00

Figures 1c and 1d display components of the Poynting vector normalized by estimates of their standard deviations. We use this robust method instead of the direct calculation of the Poynting vector because the electric waveform receivers are sometimes saturated by a strong signal. This doesn't affect measurements of phase differences which are used in our analysis. We use a Cartesian coordinate system, where the *z* axis is parallel to $\boldsymbol{B}_0$ (measured onboard by a fluxgate magnetometer), and the *x* axis lies in the plane of the local magnetic meridian and is directed away from the Earth. We can clearly see that the funnel-shaped auroral hiss emission has a negative *z* component which means that the waves are upgoing. The *x* component is mainly positive (toward higher latitudes) at higher latitudes, and negative (toward lower latitudes) at lower latitudes. This is consistent with outward propagation from a source at L∼9.7. An exception is a narrow band just below the sharp upper cutoff on the high-latitude side. Figures 1e and 1f show the direction of the wave vector determined as the normal direction to the magnetic field polarization plane using the singular value decomposition (SVD) analysis (O. Santolík, M. Parrot, and F. Lefeuvre, SVD methods for wave propagation analysis, submitted to *Radio Sci.*, 2000). The method is based on decomposition of a matrix of magnetic autopower and cross-power spectral elements at a given frequency. The results are displayed only for upward directed wave vectors. Angle θ_K (Figure 1e), representing the inclination of the wave vector from $\boldsymbol{B}_0$, shows a general trend to become more antiparallel to

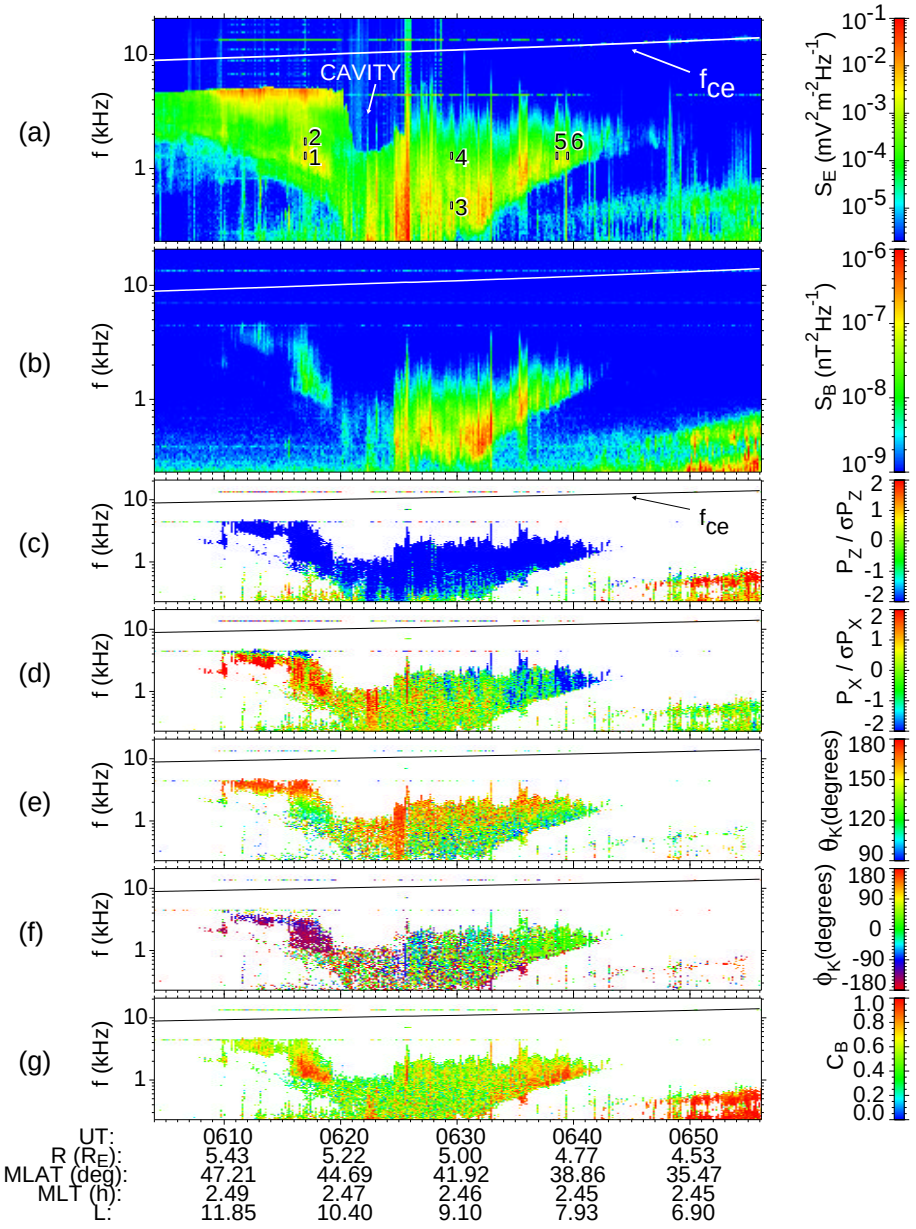

Figure 1. Detailed analysis of multicomponent data received by the high-frequency waveform receiver on March 6, 1997. (a) Spectrogram of the electric components; (b) spectrogram of the magnetic components; (c) parallel component of the Poynting vector normalized by its standard deviation; (d) the same for the component in the meridian plane; (e) angle deviation of the wave vector from $\boldsymbol{B}_0$; (f) azimuth of the wave vector measured from the meridian plane; (g) 2D degree of coherence in the magnetic polarization plane. Universal time (UT), radial geocentric distance (R) in Earth radii, the magnetic dipole latitude (MLAT) in degrees, the magnetic local time (MLT) in hours, and McIlwain's parameter (L) are on the bottom. Local electron cyclotron frequency (f_{ce}) is displayed on the spectrograms. Analysis results are shown only for a sufficiently strong signal ($S_B > 10^{-9}$ nT^2 Hz^{-1}, $S_E > 2 \times 10^{-5}$ mV^2 m^{-2} Hz^{-1}).

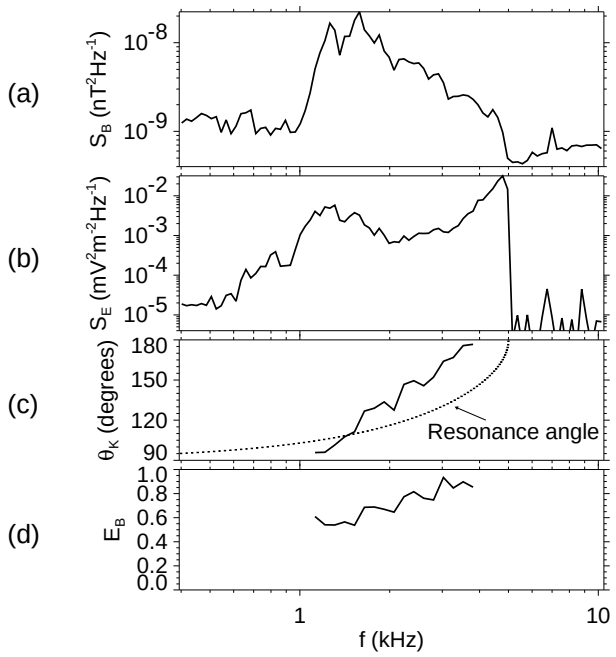

Figure 2. (a) Magnetic power spectrum taken on 0616:52 UT; (b) Simultaneously measured electric power spectrum showing a sharp upper cutoff; (c) angle deviation of the wave vector from $\boldsymbol{B}_0$ compared to the theoretical resonance angle; (d) ellipticity of the magnetic field polarization.

$\boldsymbol{B}_0$ at higher frequencies. Angle ϕ_K (Figure 1f) shows the azimuth around $\boldsymbol{B}_0$ measured from the x axis. In the high-latitude part of the funnel-shaped emission this angle is near to $\pm 180^\circ$ (wave vector points toward lower latitudes), and at lower latitudes it turns to the opposite direction. Wave vectors are thus found with different signs of their x components compared to the Poynting vectors. This relationship is consistent with the propagation pattern expected from cold plasma theory. The determination of the wave vector direction inherently supposes the presence of a single plane wave at each frequency. Strict validity of this hypothesis implies absolutely coherent field components. Figure 1g displays an estimate of the degree of coherence in the magnetic polarization plane, $C_B^2 = 2(R_{xx}^2+R_{yy}^2+2|R_{xy}|^2)/(R_{xx}+R_{yy})^2-1$, where R_{xx}, R_{yy}, and R_{xy} are the auto-power and cross-power spectra corresponding to the directions of axes of the polarization ellipse. These directions are again obtained using the SVD analysis. Higher coherence (values close to 1) is mainly observed in both high latitude and low latitude wings of the funnel, while in the central part the coherence is low. Distribution of wave energy to different wave vector directions can be thus expected in that region.

Figure 2 displays results from a single snapshot at the high-latitude side of the funnel with high C_B values. While the magnetic field power rather smoothly decreases toward higher frequencies (Figure 2a), the electric field spectrum shows a very sharp upper cutoff at ∼5 kHz (Figure 2b). Figure 2c shows that wave vector directions gradually turn from nearly perpendicular at low frequencies to nearly antiparallel in the vicinity of the higher frequency cutoff. However, they do not exactly follow the estimate of the resonance angle (dotted curve) from the cold plasma theory [*Stix*, 1992]. Figure 2d represents the ratio of the two polarization axes in the magnetic field polarization plane (ellipticity) estimated using the SVD analysis. The polarization changes from elliptical to nearly circular, while the sense of polarization is right-handed with respect to $\boldsymbol{B}_0$.

Figure 3 shows distributions of the wave energy density with respect to wave vector directions estimated by the WDF method [*Storey and Lefeuvre*, 1979]. The analysis was made in six intervals as identified in Figure 1a. WDF estimates are obtained by fitting a multi-parameter model to the auto-power and cross-power spectra of the three magnetic-field components. We use the "Model of Discrete Regions" [*Santolík and Parrot*, 2000] with an enhanced angular resolution. The model field is calculated from the cold plasma theory with 0.01° steps in θ and the WDF estimation procedure works with regions of $2.2^\circ \times 2.2^\circ$. Since we know from the previous analysis that the waves are upgoing the results are represented in a θ interval between 90° and 180°. In all the six cases the majority of wave energy is found near the resonance angle (marked by a thick dashed circle). On the high-latitude side of the funnel shape, in intervals 1 and 2, the wave vectors are found in a peak extended in the ϕ angle, but still well localized around $\phi = 210^\circ$. In the central part of the funnel (intervals 3 and 4) we observe a very broad distribution of the wave energy with respect to the ϕ angle. Local maxima are found around $\phi = 150^\circ$ and $\phi = 330^\circ$ in

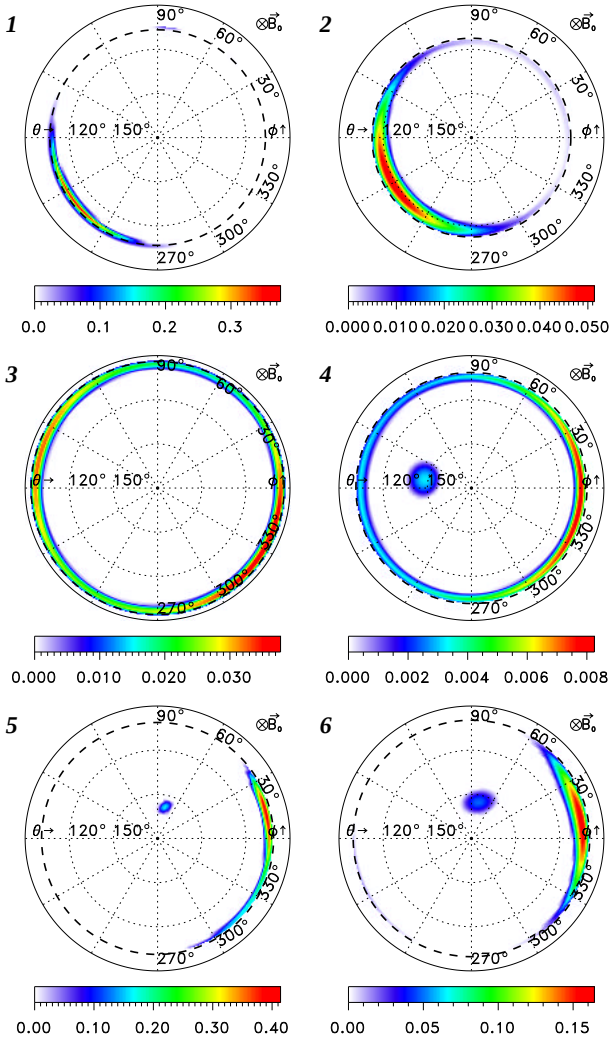

Figure 3. Polar diagrams of distributions of wave energy density with respect to the wave vector directions (WDFs). The data were analyzed in six regions in the time-frequency plane marked on the spectrograms in Figure 1. Polar angle θ shows the deviation of the wave vector from $\boldsymbol{B}_0$, zero azimuth ϕ is defined in the direction of growing magnetic latitude, at $\phi = 90^\circ$ the wave vectors point eastward. WDF values are color coded in units of 10^{-18} J m^{-3}Hz^{-1}sr^{-1}.

interval 3. At higher frequencies, in interval 4, the estimated WDF shows that a small part of the integral wave energy density (less than ∼5%) is located far from the resonance cone at $\theta \sim 150^\circ$. In the low-latitude wing of the funnel (intervals 5 and 6) we observe a similar feature, but the majority of the wave energy is found close to the resonance cone at $\phi \sim 0^\circ$.

3. Discussion

Comparing these WDF estimates with the plane wave analysis, consistent results are found on both sides of the funnel shape where the coherence is high. WDF analysis shows in more detail that the waves are concentrated near the resonance cone. Departure of the wave vector from the resonance cone in the plane-wave results at higher frequencies (Figure 2c) can be explained by a high spread of wave vectors in the azimuth (ϕ) angle. In this situation the plane-wave analysis gives an average direction which is deeper inside the resonance cone. Inversion of the *x* component of the Poynting flux just below the upper cutoff (Figure 1d) is likely a real effect. The magnetic field signal is relatively weak but the inversion is consistently observed across the high-latitude part of the emission. It is probably connected to propagation effects taking place near the cutoff but a detailed ray tracing study is beyond the scope of this letter.

A very small fraction of integral energy density is found far from the resonance cone in the last three WDF estimates (Figure 3, intervals 4–6). This deviation is probably an artifact of the method but we cannot completely exclude the possibility that such a small fraction of waves really propagates with wave vectors nearly antiparallel to $\boldsymbol{B}_0$. However, since no such results are obtained at higher latitudes before 0625 UT, they are likely connected to the presence of hot plasma which is observed at plasma sheet energies after 0625 UT by the Hydra plasma analyzer [*Scudder et al.*, 1995] (recall that no hot plasma effects are included in the model used for the WDF estimation). Although the cold plasma theory seems to be sufficient to describe the main propagation properties of the observed hiss emissions, a detailed study of wave dispersion, involving hot plasma measurements, will be helpful to understand these details.

In the central part of the hiss emission the waves are coming from different azimuth angles (Figure 3, intervals 3–4). Although some finite width of the distribution in ϕ angle is always connected to finite resolution of the WDF estimation, the results clearly show the difference between the central part and the wings of the funnel. The peak values are also displaced in azimuth from the results obtained at higher latitudes. Our observations are thus rather consistent with an extended sheet source region, probably elongated in the longitudinal direction. From such a source region the waves arrive at different azimuth angles to the spacecraft. This would not be possible from a vertical line or point source.

The longitudinaly extended sheet source is consistent with the traditional attribution of the source of VLF saucers and upgoing funnel-shaped hiss to the region of downward currents [*James*, 1976; *Gurnett et al.*, 1983]. Recent observations of the FAST spacecraft at altitudes of ≈4000 km show that this region contains upgoing and counterstreaming energetic electrons [*McFadden et al.*, 1999]. Since we observe the waves well above the source, local particle measurements are difficult to use for examination of the origin of hiss. However, investigation of its propagation pattern from multicomponent wave measurements proves to be useful for a remote characterization of the source geometry.

Acknowledgments. We warmly thank J. S. Pickett and J. Dowell who designed and developed the preprocessing and calibration software for the HFWR data, and J. Scudder who made accessible the Hydra particle data through Papco. We gratefully acknowledge L. R. O. Storey for helpful discussions. This work was supported by the NASA Goddard Space Flight Center under Grant No. NAG5-7943. O. Santolík thanks the Fulbright commission in Prague for support during his stay in Iowa, and acknowledges the support of the Czech Grant Agency grant 205/01/1064.

References

Gurnett, D. A., A satellite study of VLF hiss, *J. Geophys. Res.*, *71*, 5599–5615, 1966.

Gurnett, D. A., and L. A. Frank, VLF hiss and related plasma observations in the polar magnetosphere, *J. Geophys. Res.*, *77*, 172–190, 1972.

Gurnett, D. A., S. D. Shawhan, and R. R. Shaw, Auroral hiss, Z mode radiation, and auroral kilometric radiation in the polar magnetosphere: DE 1 observations, *J. Geophys. Res.*, *88*, 329–340, 1983.

Gurnett, D. A., A. M. Persoon, R. F. Randall, D. L. Odem, S. L. Remington, T. F. Averkamp, M. M. DeBower, G. B. Hospodarsky, R. L. Huff, D. L. Kirchner, M. A. Mitchell, B. T. Pham, J. R. Phillips, W. J. Schintler, P. Sheyko, and D. Tomash, The Polar Plasma Wave Instrument, *Space Sci. Rev.*, *71*, 597–622, 1995.

James, H. G., VLF saucers, *J. Geophys. Res.*, *81*, 501–514, 1976.

Kasahara, Y., K. Yoshida, T. Matsuo, I. Kimura, and T. Mukai, Propagation characteristics of auroral hiss observed by Akebono satellite, *J. Geomag. Geoelectr.*, *47*, 509–525, 1995.

McFadden, J. P., C. W. Carlson, and R. E. Ergun, Microstructure of the auroral acceleration region as observed by FAST, *J. Geophys. Res.*, *104*, 14,453–14,480, 1999.

Mosier, S. R., and D. A. Gurnett, VLF measurement of the Poynting flux along the magnetic field with the Injun 5 satellite, *J. Geophys. Res.*, *74*, 5675–5687, 1969.

Persoon, A. M., D. A. Gurnett, W. K. Peterson, J. H. Waite, Jr., J. L. Burch, and J. L. Green, Electron density depletions in the nightside auroral zone, *J. Geophys. Res.*, *93*, 1871–1895, 1988.

Santolík, O., and M. Parrot, Application of wave distribution function methods to an ELF hiss event at high latitudes, *J. Geophys. Res.*, *105*, 18,885–18,894, 2000.

Scudder, J. D., F. Hunsaker, G. Miller, J. Lobell, T. Zawistowski, K. W. Ogilvie, J. Keller, D. Chornay, F. Herrero, R. Fitzenreiter, D. Fairfield, J. Needell, D. Bodet, J. Googins, C. Kletzing, R. Torbert, J. Vandiver, R. Bentley, W. Fillius, C. McIlwain, E. Whipple, and A. Korth, Hydra - a three dimensional electron and ion instrument for the Polar spacecraft of the GGS mission, *Space Sci. Rev.*, *71*, 459–495, 1995.

Stix, T. H., *Waves in Plasmas*, Am. Inst. of Phys., New York, 1992.

Storey, L. R. O., and F. Lefeuvre, The analysis of 6-component measurements of a random electromagnetic wave field in a magnetoplasma, 1, The direct problem, *Geophys. J. R. Astron. Soc.*, *56*, 255–270, 1979.

D. A. Gurnett, Department of Physics and Astronomy, University of Iowa, Iowa City, IA 52242-1479, U.S.A. (gurnett@space.physics.uiowa.edu)

O. Santolík, Faculty of Mathematics and Physics, Charles University, V Holešovičkách 2, CZ-18000 Praha 8, Czech Republic. (ondrej.santolik@mff.cuni.cz)

(Received June 13, 2001; revised September 21, 2001;
accepted October 25, 2001; published May 31, 2002.)